Supporting Information for:

Direct Relationship Between Increased Expression and Mistrafficking of the Charcot-Marie-Tooth-Associated Protein PMP22

Justin T. Marinko[a,b], Bruce D. Carter[a,c] Charles R. Sanders[a,b,d,1]

[a] *Department of Biochemistry, Vanderbilt University, Nashville, TN, 37240 USA*

[b] *Center for Structural Biology, Vanderbilt University, Nashville, TN, 37240 USA*

[c] *Vanderbilt Brain Institute, Nashville, TN, 37240 USA*

[d] *Department of Medicine, Vanderbilt University Medical Center, Nashville, TN, 37232 USA*

This PDF Contains:

Supporting Information Fig. S1-S5

Supporting Information Tables S1-S6 are submitted as separate Excel Files

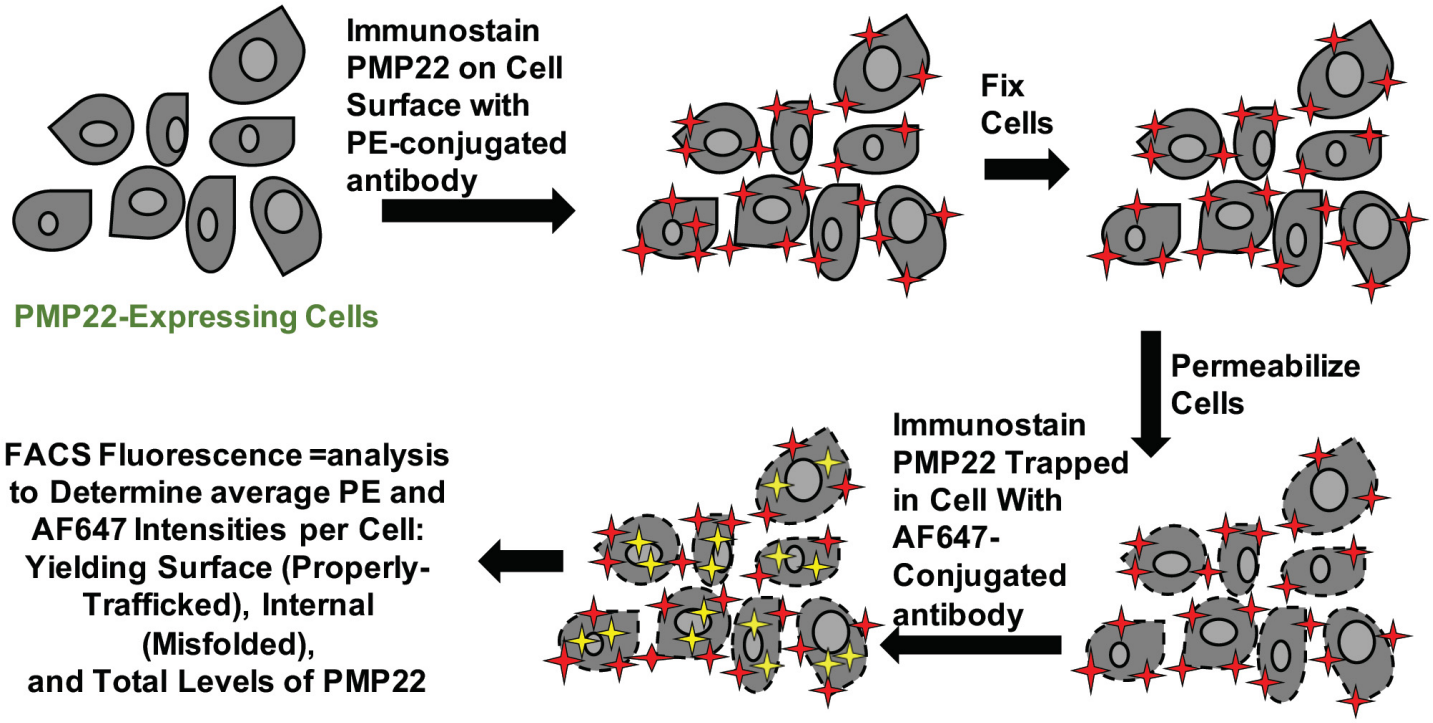

Figure S1. Summary of the trafficking assay used in this work. Briefly, cells were harvested and incubated with a primary myc antibody conjugated to phycoerythrin (PE) which labels cell surface PMP22. Cells were then washed, fixed, and permeabilized and again incubated with a primary myc antibody this time conjugated to AlexaFluora647 (AF647) which labels internal PMP22. PMP22 trafficking can then be analyzed in individual cells using flow cytometry. Trafficking efficiency is defined as the normalized fluorescent intensity on the PE channel divided by the sum of the normalized fluorescent intensities of the PE and AF647 channels.

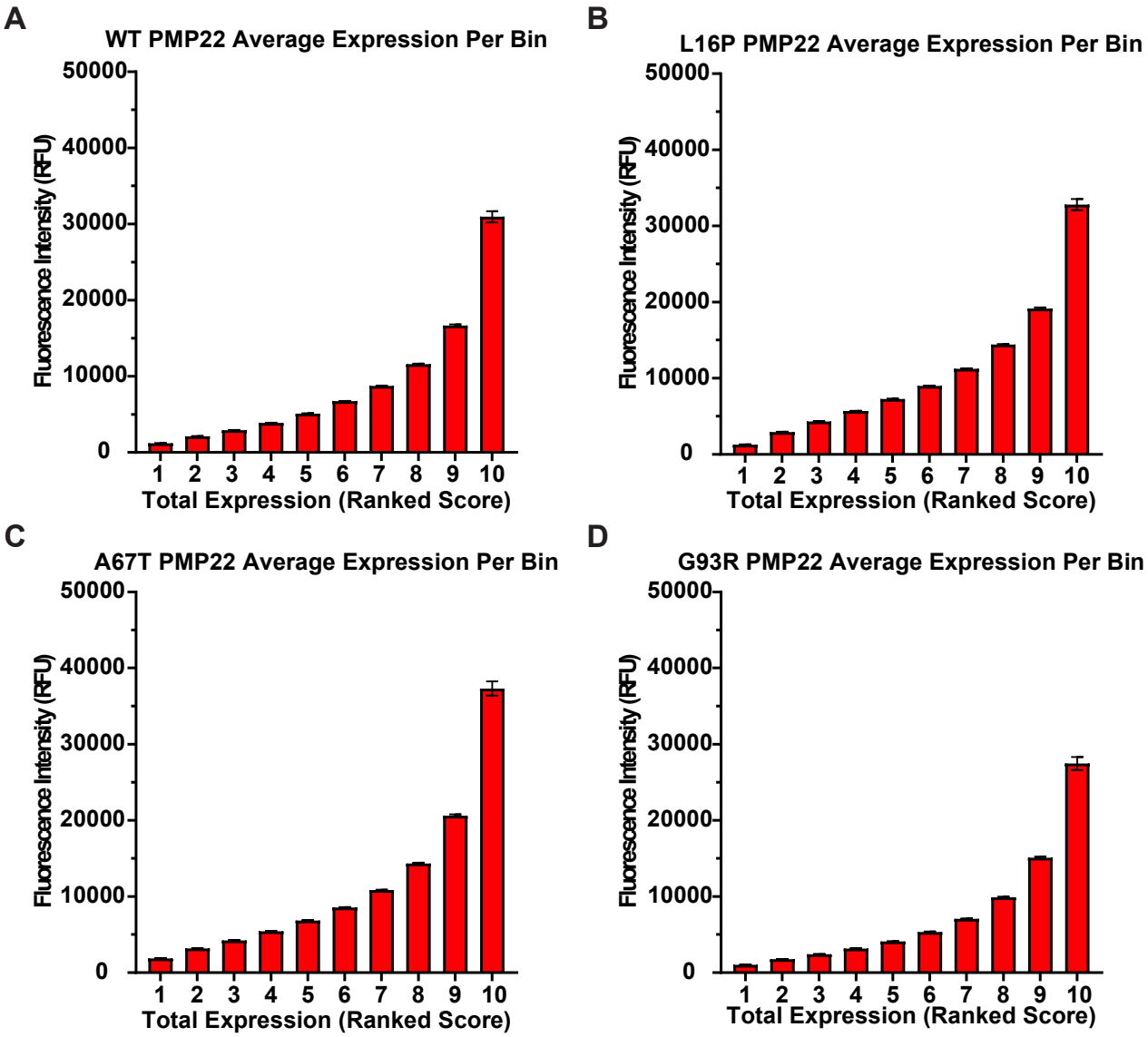

Figure S2. The mean total PMP22 expression levels (±95% confidence interval) of the 750 cells in each bin is shown for transiently transfected cells expressing WT, L16P, A67T or G93R PMP22. Data is from three independent biological replicates.

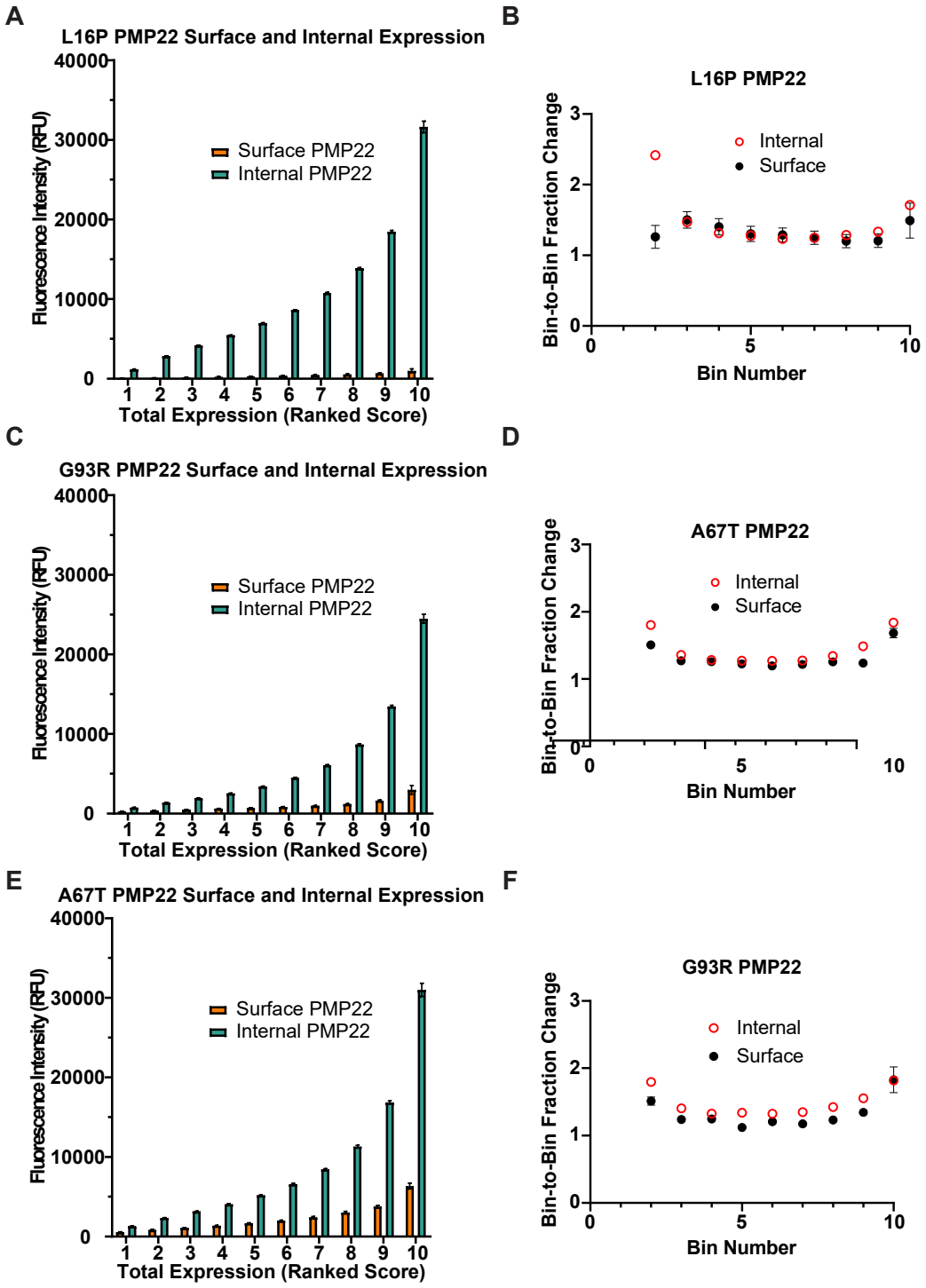

Figure S3. Trafficking efficiency values plotted in **Figure 3** were deconvoluted and the mean levels of cell surface PMP22 (orange) and of internal PMP22 (green) ± 95% confidence interval (CI) are plotted for each bin for L16P **(A)**, A67T **(C)** and G93R **(E)** PMP22. **(B, D, and F)** The fraction change of relative fluorescence

between each bin (bin 2/bin1, bin 3/bin2…bin10/bin 9) was calculated for both cell surface (black circles) and internal (open red circles) PMP22 shown in A, C, and E. Mean fraction change is reported ± 95% confidence interval (CI) (for values with no visible error bars the error was too small to be represented by bars).

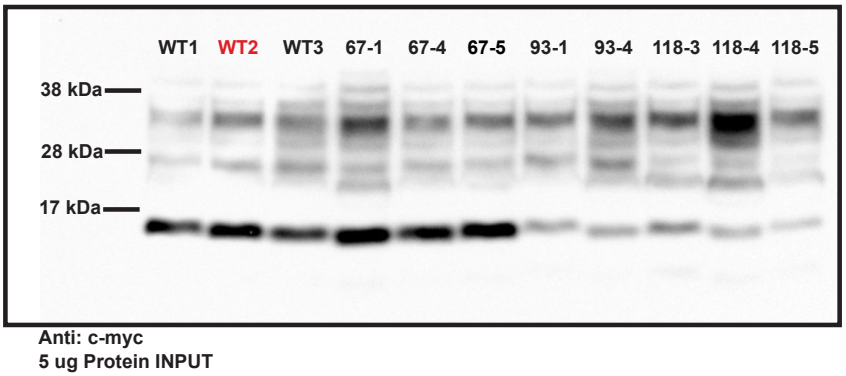

Figure S4. Western blot used to confirm the generation of PMP22 stable expressor 293 cells. WT-2 (shown in red) was the clone that was used in this work. 5 ug of total protein lysates were loaded onto SDS-PAGE gels and PMP22 was identified using an anti-myc antibody.

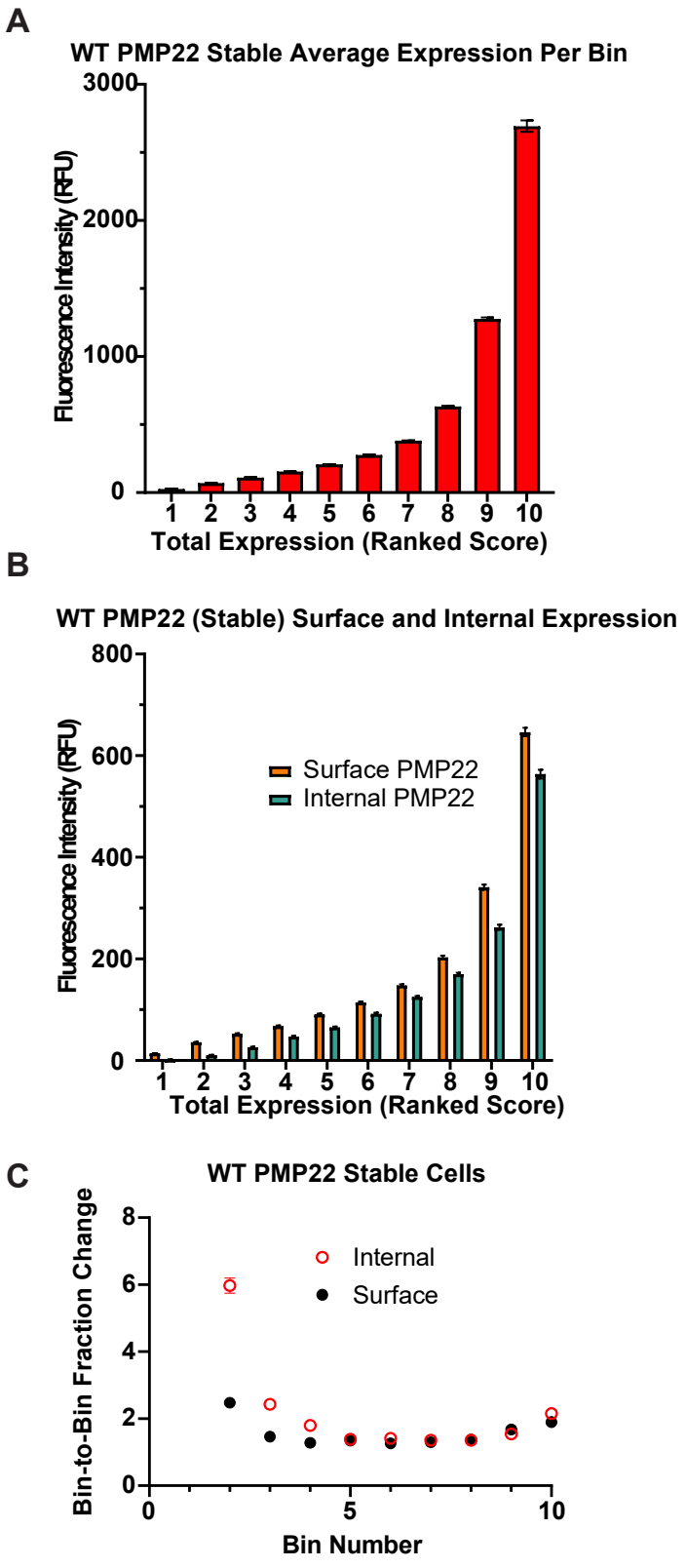

Figure S5. (A) The mean total PMP22 expression levels (±95% confidence interval) of the 2296 cells in each bin is shown for HEK293 cells stably expressing WT PMP22 from two independent biological replicates. **(B)**

Trafficking efficiency values plotted in **Figure 4** were deconvoluted and the mean levels of cell surface PMP22 (orange) and of internal PMP22 (green) ± 95% confidence interval (CI) are plotted for each bin. **(C)** The fraction change of relative fluorescence between each bin (bin 2/bin1, bin 3/bin2…bin10/bin 9) was calculated for both cell surface (black circles) and internal (open red circles) PMP22 shown in B. Mean fraction change is reported ± 95% confidence interval (CI) (for values with no visible error bars the error was too small to be represented by bars).

Table S1. Raw data for WT PMP22 trafficking in HEK293 cells
Table S2. Raw data for WT PMP22 trafficking in MDCK cells
Table S3. Raw data for L16P PMP22 trafficking in HEK293 cells
Table S4. Raw data for A67T PMP22 trafficking in HEK293 cells
Table S5. Raw data for G93R PMP22 trafficking in HEK293 cells
Table S6. Raw data for WT PMP22 trafficking in HEK293 stable expressor cells